Available online at www.sciencedirect.com
SCIENCE DIRECT®
International Journal of Mass Spectrometry 241 (2005) 99–108
International Journal of Mass Spectrometry
www.elsevier.com/locate/ijms

Dissociation reactions of diatomic silver cations with small alkenes: experiment and theory

Manuel J. Manard, Paul R. Kemper, Catherine J. Carpenter, Michael T. Bowers*

Department of Chemistry and Biochemistry, University of California, Santa Barbara, CA 93106, USA

Received 4 November 2004; accepted 16 December 2004

Abstract

Reaction of ground-state Ag_2^+ ($^2\Sigma_g^+$, $4d^{20}\,\sigma(5s)^1$) with either ethene or propene leads to both simple ligand addition and loss of neutral Ag to form ligated Ag^+. Rate constants for the dissociation of Ag_2^+ via association of both ethene and propene have been measured. Experimental and theoretical analysis suggests that loss of a neutral Ag atom occurs upon addition of either the second ethene or first propene ligand to the Ag_2^+ ion. The measured rate constants exhibit a negative temperature dependence and relatively high reaction efficiency suggesting that the dissociation reactions are exothermic. Electronic structure calculations were preformed using density functional theory (DFT) at the B3LYP level in order to generate potential transition state structures for the dissociation reactions. Phase space theory (PST) was used to model the experimental rate data. Good agreement was found between experiment, DFT calculations and PST results for both systems. In both reactions, the negative temperature dependence is due to two factors: The reactions are only mildly exothermic and the product density of states increases more slowly with energy than the reactant density of states. The second factor is due to an atom being one of the products. No evidence for tight transition states was found for either reaction.

Keywords: Dissociation reaction; Silver cation clusters; Small alkene

1. Introduction

Reactions involving bare transition metal ions with small molecules have received considerable attention over the past few decades [1]. Systematic experiments have examined the properties of an assortment of gas-phase metal ion M_y^+–X_n clusters with X = H_2 [2–12], CO [13–18], O_2 [19,20], and CH_4 [3,21–24], along with a variety of other ligands [25–29]. These experiments have proven essential in broadening our understanding of the nature of transition metal ion bonding. Of particular interest is sigma bond activation in small hydrocarbons due to possible catalytic conversion processes. Activation of C–H and C–C bonds by atomic transition metal ions was first shown to be possible by the experiments of Allison et al. [30]. Numerous subsequent experimental studies have focused on gas-phase transition metal ions interacting with small hydrocarbons [21,22,24,28,31–36]. These investigations, coupled with theoretical calculation, have provided fundamental information, such as metal-ligand bond dissociation energies (BDEs), geometries, and bonding interactions, that is necessary to elucidate the underlying factors involved in catalytic processes.

Small alkenes have been the focus of many studies because of their ability to serve as effective prototypes for other unsaturated hydrocarbons [37–41]. Dewar first proposed that metal-olefin bonding consists mainly of electron density donated from the π orbitals of the ligand to an unoccupied s orbital on the metal coupled with back-donation from filled d orbital of the metal to an unoccupied π^* orbitals of the ligand [42]. Subsequently, many others have used this model to explain the bonding of small alkenes to group 11 transition metal cations [37,38,40], to which Dewar's model would be expected to be particularly applicable. Furthermore, it has

* Corresponding author. Tel.: +1 805 893 2893; fax: +1 805 893 8703.
E-mail address: bowers@chem.ucsb.edu (M.T. Bowers).

1387-3806/$ – see front matter © 2005 Elsevier B.V. All rights reserved.
doi:10.1016/j.ijms.2004.12.025

been shown that back-donation plays a more significant role in the bonding of first row transition metals and is less important for the second and third row counterparts [40,41,43].

Recently, there has been increased interest in the interactions of group 11 coinage metals with ethene and propene due to the discovery that clusters of Ag on semiconductor surfaces can serve as epoxidation catalysts for these alkenes [44]. At UCSB, we have recently initiated a program to elucidate the detailed mechanisms of these reactions using size-selected silver and gold clusters on titanium oxide surfaces. As part of that program, investigations into the chemistry of positively and negatively charged silver and gold clusters with propene and ethene in the gas-phase have also commenced. Here, we report our first results using $Ag^+(4d^{10})$ and $Ag_2^+(4d^{20}\ \sigma(5s)^1)$ cations as reagents. Previously, Guo and Castleman [37] measured the binding energies of one and two C_2H_4 ligands to Ag^+. Chen and Armentrout [36] examined reactions of Ag^+ with a variety of small hydrocarbons and reported a lower limit for the BDE of the $Ag^+(C_2H_4)$ ion. No prior studies of Ag_2^+ reacting with either C_2H_4 or C_3H_6 have been reported. In this paper, we present an experimental and theoretical investigation of the kinetics of Ag^+ and Ag_2^+ reacting with C_2H_4 and C_3H_6. Equilibrium studies leading to the determination of bond dissociation energies will be reported in the accompanying paper [45].

2. Experimental methods

A description of the instrument and experimental details has been given previously [5,7,46], and only a brief description will be given here. The silver ions are generated by pulsed laser vaporization of a translating/rotating silver rod in a high-pressure Ar bath gas. Clusters exiting the source are mass selected by a quadrupole mass filter and injected into a 4 cm long drift/reaction cell containing a mixture of reactant gas (either C_2H_4 or C_3H_6) and He. The typical composition of the gas mixture is 4.5 Torr of He combined with 0.01–0.05 Torr of either C_2H_4 or C_3H_6. Ag_m^+ ions are drawn through the cell by a weak electric field, which is small enough that the thermal energy of the ions is not significantly perturbed. The amount of time the ions spend in the cell can be controlled by adjusting the drift voltage and cell pressure. The maximum drift voltage used in this study was approximately 40 V. Ions leaving the cell pass through a second quadrupole mass filter and are detected. Association reactions resulting in the formation of $Ag_m^+L_n$ clusters reach equilibrium quickly, as verified by noting the relative intensities of the product and reactant ions remain unchanged as drift time is varied. For reactions not at equilibrium, ion intensities can be measured as a function of drift time to obtain rate constants [47].

3. Experimental results

Mass spectra of the Ag_m^+ ($m = 1$–3) clusters acquired at 300 K are shown in Figs. 1–3, respectively. The spectrum

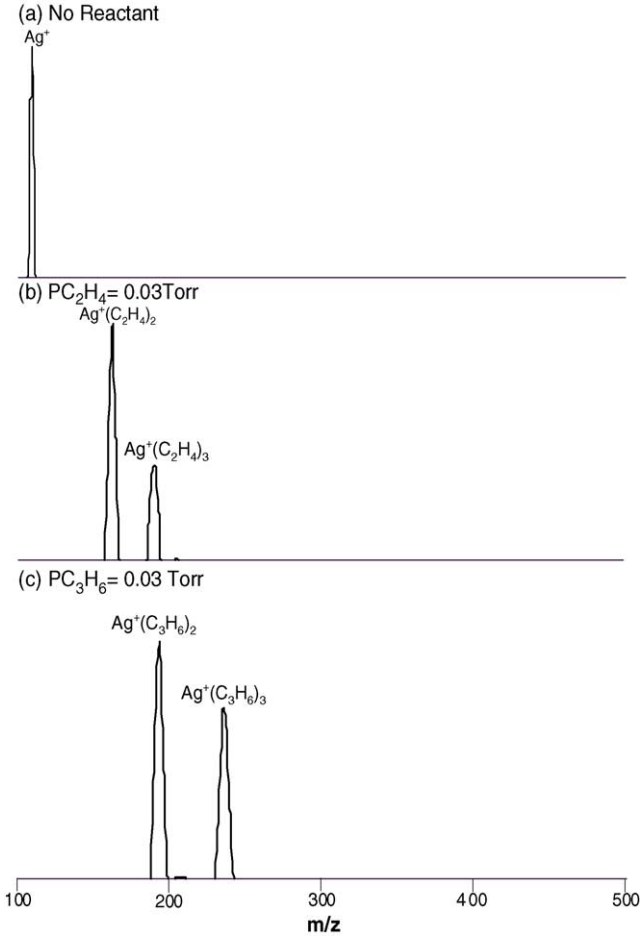

Fig. 1. Mass spectra of Ag^+ at different reactant gas pressures at 300 K. (a) No C_2H_4 was added; (b) 0.03 Torr of C_2H_4 gas added; (c) 0.03 Torr of C_3H_6 gas added. In all cases, there was 4.5 Torr of He in the reaction cell.

shown in panel (a) of each figure was recorded without the addition of a reactant gas to the drift cell. As expected, only the bare transition metal peaks are observed. Panel (b) was recorded after the addition of ethene to the drift cell (0.01–0.03 Torr) and panel (c) was recorded after the addition of propene (0.01–0.03 Torr). Fig. 1b and c and Fig. 3b and c show that the only chemistry Ag^+ and Ag_3^+ undergo in the presence of either alkene reactant is simple clustering (Eq. (1) where L = C_2H_4 and C_3H_6).

$$Ag_{1,3}^+L_{n-1} + L \rightleftarrows Ag_{1,3}^+L_n \quad (1)$$

No products associated with the fragmentation of Ag_3^+ are observed in Fig. 3b and c. The chemistry observed in the Ag_2^+ system, however, is not restricted to clustering. Panels (b) and (c) of Fig. 2 show the presence of $Ag^+(C_2H_4)_n$ and $Ag^+(C_3H_6)_n$ fragments, respectively, in addition to Ag_2^+-alkene clusters. The observations for this system are summarized by Eq. (2) (L = C_2H_4 and C_3H_6).

$$Ag_2^+(L)_{n-1} + L \underset{k_{-a}(T)}{\overset{k_a(T)}{\rightleftarrows}} Ag_2^+(L)_n \quad (2a)$$

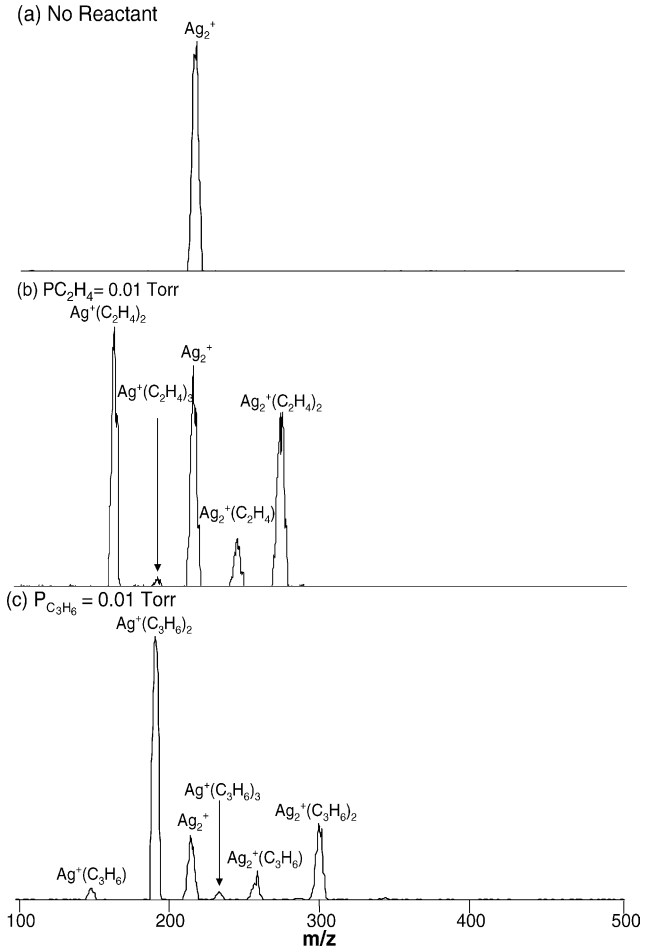

Fig. 2. Mass spectra of Ag_2^+ at different reactant gas pressures at 300 K. (a) No C_2H_4 was added; (b) 0.01 Torr of C_2H_4 gas added; (c) 0.01 Torr of C_3H_6 gas added. In all cases, there was 4.5 Torr of He in the reaction cell.

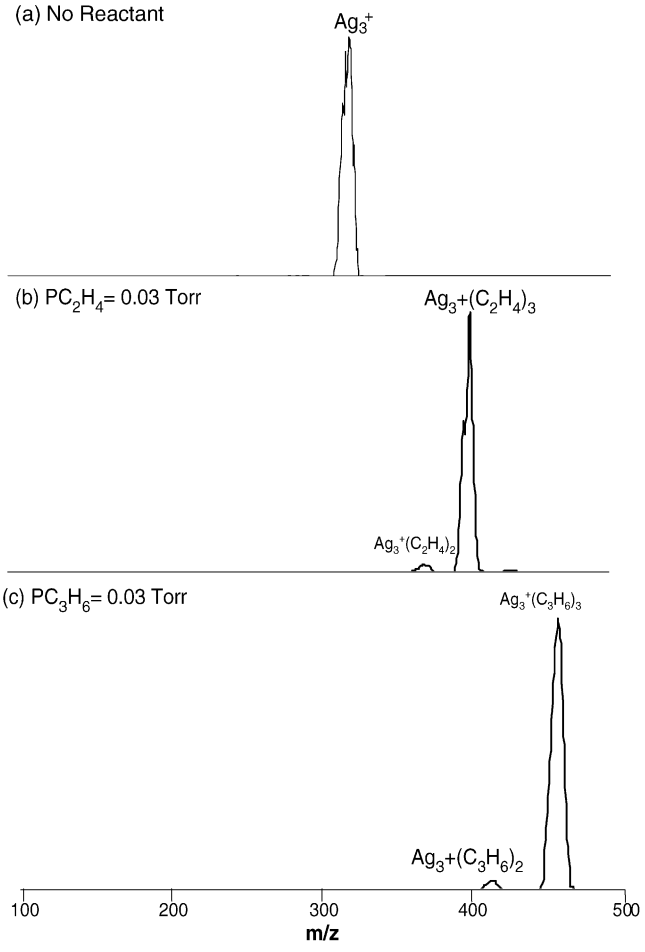

Fig. 3. Mass spectra of Ag_3^+ at different reactant gas pressures at 300 K. (a) No C_2H_4 was added; (b) 0.03 Torr of C_2H_4 gas added; (c) 0.03 Torr of C_3H_6 gas added. In all cases, there was 4.5 Torr of He in the reaction cell.

$$Ag_2^+(L)_{n-1} + L \xrightarrow{k_r(T)} Ag^+(L)_n + Ag \quad (2b)$$

Due to the fact that only Ag_2^+ ions are initially injected into the drift cell, the observed fragments can only be products of the dissociation of Ag_2^+. Furthermore, with the exception of the addition of the reactant gases, the experimental conditions at which the three spectra in Fig. 2 were obtained remained constant. This suggests that the dissociation of Ag_2^+ occurs by association of C_2H_4 and C_3H_6, rather than via other routes such as CID since (1) the pressures of the alkene gases (0.01 Torr) are relatively small in comparison to that of He (4.5 Torr) and (2) no Ag^+ fragments are observed in the spectra when only He is present in the drift cell (see Fig. 2).

In our experiment, comparable amounts of $Ag^+(L)_n$ dissociation and $Ag_2^+(L)_n$ association products are formed in the Ag_2^+/L systems, although the relative amounts vary with temperature. Because the association reactions (Eqs. (1) and (2a)) are at equilibrium, temperature-dependent experiments are used to determine BDEs. The values relevant to the present discussion are summarized in Table 1. As noted, a complete discussion of these bond energies will be presented elsewhere [45]. Literature values for loss of a neutral Ag atom from both Ag_2^+ and Ag_3^+ are available: 36.2 ± 0.7 kcal/mol [48] and 40.1 ± 2.0 kcal/mol [49] for Ag_2^+ and 62.3 ± 3.2 kcal/mol [49] for Ag_3^+.

Rate constants for the dissociation of Ag_2^+ (Eq. (2b)) are reported here. The rate constants measured for both the C_2H_4 and C_3H_6 systems were invariant to changes in the reactant gas pressures within the limited pressure range accessible in our experiment (0.01–0.05 Torr).

Table 1
Thermochemistry summary for $Ag_m^+(L)_{n-1} + L \rightleftarrows Ag_m^+(L)_n$

m	n	L = C_2H_4		L = C_3H_6	
		$-\Delta H_0^{\circ}$ [a]	D_0 [b]	$-\Delta H_0^{\circ}$ [a]	D_0 [b]
1	1	32.2 ± 3.0	31.24	39.2 ± 3.0	35.02
1	2	30.1 ± 1.3	26.10	32.9 ± 1.5	27.30
2	1	24.7 ± 1.5	20.86	28.1 ± 1.5	23.52
2	2	22.5 ± 1.3	16.19	25.8 ± 1.5	17.48

[a] Values from Ref. [45] obtained by fitting experimental data with theoretical vibrational frequencies, rotational constants and geometries, in units of kcal/mol.

[b] From DFT calculation, in units of kcal/mol.

4. Reaction mechanism

One of the issues of interest is the number of C_2H_4 and C_3H_6 ligands needed to initiate the dissociation reactions of Ag_2^+. For C_3H_6, the data in Fig. 2c indicate that at 300 K, $Ag^+(C_3H_6)_2$ is the dominant species with small amounts of $Ag^+(C_3H_6)$ and $Ag^+(C_3H_6)_3$ also present. If the reaction time is substantially increased, $Ag^+(C_3H_6)$ disappears and $Ag^+(C_3H_6)_3$ increases in relative intensity. Continued increase in reaction time eventually results in no change in the $Ag^+(C_3H_6)_2$ and $Ag^+(C_3H_6)_3$ relative intensities, indicating the system has come to equilibrium. Hence, the $Ag^+(C_3H_6)$ ions seen at short times must be a primary reaction product caused by the dissociation reaction,

$$Ag_2^+ + C_3H_6 \rightleftarrows [Ag_2^+C_3H_6]^* \rightarrow Ag^+(C_3H_6) + Ag \quad (3)$$

and not back dissociation of $Ag^+(C_3H_6)_2$. Thus, we conclude that a single C_3H_6 ligand is sufficient to induce the dissociation reaction.

The situation is different for the C_2H_4 ligand. In this case, $Ag^+(C_2H_4)$ is never observed at 300 K and $Ag^+(C_2H_4)_2$ is the smallest Ag^+-ligated species (see Fig. 2b). Again, at long times the system comes to equilibrium but no $Ag^+(C_2H_4)$ appears. We conclude the dominant dissociation reaction is shown in Eq. (4).

$$Ag_2^+(C_2H_4) + C_2H_4 \rightleftarrows [Ag_2^+(C_2H_4)_2]^* \rightarrow Ag^+(C_2H_4)_2 + Ag \quad (4)$$

Therefore, one C_3H_6 ligand is sufficient for dissociation of Ag_2^+ but two C_2H_4 ligands are required.

Rate constants for the pseudo-first order reactions (3) and (4) were determined from the expression given in Eq. (5) where $k_r(T)$ is given in reaction (2b):

$$\ln\left[\frac{\sum Ag_2^+(\text{unreacted})}{\sum Ag^+(\text{containing})}\right] = -k_r(T) \times \rho(L) \times t \quad (5)$$

In Eq. (5), $\Sigma[Ag_2^+(\text{unreacted})]$ is the sum of the concentrations of the unreacted Ag_2^+ reactant species (Ag_2^+ and $Ag_2^+(C_2H_4)$ for $L = C_2H_4$ and Ag_2^+ for $L = C_3H_6$), $\Sigma[Ag^+(\text{containing})]$ is the sum of the concentrations of all Ag^+-containing ions, and $\rho(L)$ is the number density of the reactant gas in the drift cell at a given pressure and temperature. The concentrations used in Eq. (5) are directly proportional to the peak intensities in the mass spectra measured after the ions exit the cell. Rate constants for the overall reaction of Ag_2^+ were determined by varying the amount of time the Ag_2^+ ions spend in the drift cell and plotting the left-hand side of Eq. (5) as a function of time. The resulting plots are approximately linear with slopes that are proportional to $k_r(T)$. An example of such a plot is given in supporting information.

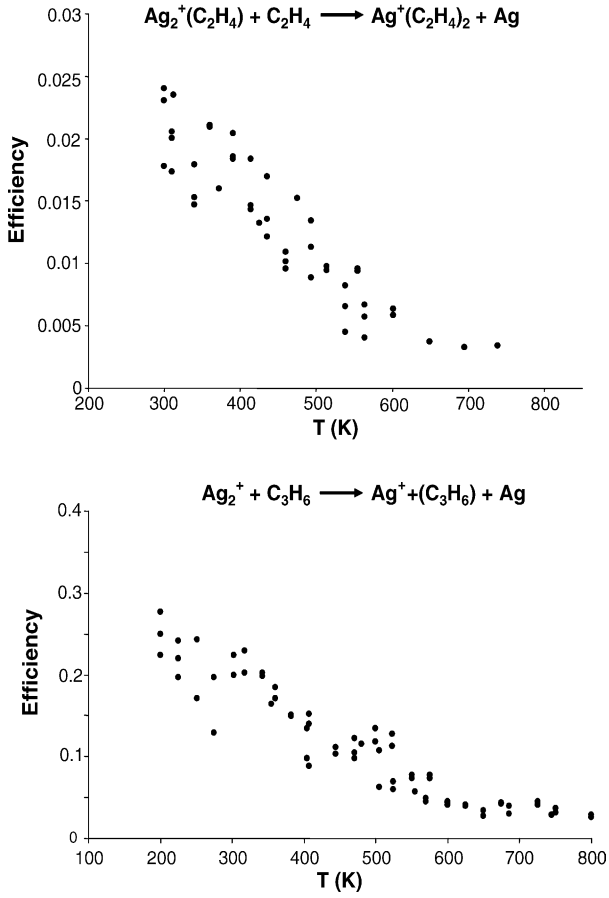

Fig. 4. Experimental reaction efficiencies for Ag_2^+ reacting with C_2H_4 and C_3H_6 as a function of temperature. For details of analysis see text.

The experimental rate constant can be used to calculate the reaction efficiency $\omega(T)$ given by Eq. (6),

$$\omega(T) = \frac{k_r(T)}{k_{coll}} \quad (6)$$

where k_{coll} is the collisional rate constant obtained from Langevin theory. The reaction efficiencies were determined over a wide range of temperature and the results are plotted in Fig. 4.

5. Theory

The product ions were all examined theoretically to determine the molecular parameters needed to analyze the experimental data and to identify factors important in the reaction of Ag_2^+ with ethene and propene. DFT calculations [50] were carried out using the B3LYP hybrid functional [51,52], and the Gaussian 98 package [53]. For all of the calculations reported here, carbon and hydrogen were described using the standard 6-31 + G** basis set [54]. The basis set for silver is a (5s6p4d)/[3s3p2d] contraction of the Hay–Wadt ($n + 1$) effective core potential (ECP) valence double zeta basis proposed by Hay [55,56]. Here, the outermost core orbitals are

not replaced by the ECP, but are instead treated equally with the valence orbitals. This allows for increased accuracy in the calculations without a substantial increase in computation time. The ECP for silver incorporates the Darwin and mass–velocity relativistic effects into the potential.

Geometry optimizations of all of the observed silver-alkene clusters were performed over a wide range of geometries in order to determine a true global minimum. All confirmed minima consist of largely unperturbed C_2H_4 and C_3H_6 ligands bound to a metal core ion. Vibrational frequencies were calculated for all minima.

The reaction efficiencies for the dissociation reactions were studied using statistical phase space theory (PST) [57,58]. Input parameters for the PST calculations including cluster geometries, vibrational frequencies, rotational constants and relative energies were taken from DFT calculations.

To calculate the reaction efficiency using PST, three species along the reaction coordinate were taken into account: the reactant orbiting transition state (OTS_R), the product orbiting transition state (OTS_P) and a possible tight transition state between the two orbiting transition states, Eq. (7).

$$Ag_2{}^+L_{n-1} + L \overset{OTS_R}{\rightleftarrows} Ag_2{}^+L_n \overset{TTS}{\rightleftarrows} (Ag)Ag^+L_n \overset{OTS_P}{\longrightarrow} Ag^+L_n + Ag \quad (7)$$

The efficiency depends on the sums of rotational and vibrational states at these transition states. It can be shown [57a,b] that the efficiency at a given energy E and angular momentum J is given by Eq. (8), where for the sake of brevity, the E and J arguments have been left off the terms on the right-hand side of the equation.

$$\omega_{PST}(E, J) = \frac{N^P_{OTS}}{N^P_{OTS} + N^R_{OTS} + (N^P_{OTS}N^R_{OTS}/N_{TTS})} \quad (8)$$

In this expression, N^P_{OTS} is the sum of states at E and J for the OTS_P, N^R_{OTS} is the sum of states at E and J for the OTS_R and N_{TTS} is the sum of states at E and J for the TTS. To obtain the overall reaction efficiency $\omega_{PST}(T)$, $\omega_{PST}(E, J)$ is integrated over the E and J distribution of the chemically activated reactant complex $Ag_2{}^+(L)_n$. The reaction efficiencies calculated with PST can then be compared to those measured under the conditions of our experiment.

6. Discussion

The data in Fig. 2b and c are strongly suggestive that addition of the first C_3H_6 ligand to $Ag_2{}^+$ provides sufficient energy to form $Ag^+(C_3H_6)$ + Ag products but it takes two C_2H_4 ligands to accomplish the analogous dissociation reaction. It is instructive to see if thermochemistry alone can account for these observations. First, consider the C_3H_6 system and the following reactions:

$$Ag_2{}^+ + C_3H_6 \rightarrow Ag^+(C_3H_6) + Ag \quad (9)$$

$$Ag_2{}^+ \rightarrow Ag^+ + Ag \quad (9a)$$

$$Ag^+ + C_3H_6 \rightarrow Ag^+(C_3H_6) \quad (9b)$$

The sum of reactions (9a) and (9b) yield reaction (9). The association energy for reaction (9b) has been measured to be 39.2 ± 3.0 kcal/mol [45] (Table 1). The overall reaction energy, ΔH_{rxn} (9) = $D_0(Ag^+–Ag) - 39.2 \pm 3.0$ kcal/mol, is the sum of the reaction energies of reactions (9a) and (9b). Hence, if $D_0(Ag^+–Ag) < 39.2$ kcal/mol, then reaction (9) is exothermic and simple thermochemistry could explain our experimental observation. There are two experimental values for $D_0(Ag^+–Ag)$; Beutel et al. [48], using photoionization of a cold Ag_2 molecular beam, obtained a value of 36.2 ± 0.7 kcal/mol. Kruckeburg et al. [49] obtained a value of 40.1 ± 2.0 kcal/mol using multiple-collision induced dissociation in a Penning trap. We have calculated $D_0(Ag^+–Ag)$ using DFT and obtained 36.24 kcal/mol. The Beutel et al. value and our DFT value clearly indicate that reaction (9) is exothermic. The Kruckeburg et al. value also does so within the error limits of the values but is probably a bit too high to rationalize our experimental observations. Overall, thermochemistry nicely supports dissociation of $Ag_2{}^+$ with the addition of the first C_3H_6 ligand.

A similar set of reactions for the ethene ligand is given in the following:

$$Ag_2{}^+ + C_2H_4 \rightarrow Ag^+(C_2H_4) + Ag \quad (10)$$

$$Ag_2{}^+ \rightarrow Ag^+ + Ag \quad (10a)$$

$$Ag^+ + C_2H_4 \rightarrow Ag^+(C_2H_4) \quad (10b)$$

In this case, $D_0(Ag^+–Ag)$ must be less than 32.2 ± 3.0 kcal/mol for the reaction to be exothermic. Both the experimental and DFT values for $D_0(Ag^+–Ag)$ indicate that reaction (10) is endothermic, probably by about 4.0 kcal/mol. If a second C_2H_4 ligand is added, an additional 30.1 ± 1.3 kcal/mol becomes available (Table 1). This makes the dissociation reaction overwhelmingly exothermic. However, this is an unrealistic situation since the intermediate $Ag_2{}^+(C_2H_4)$ ion is almost certainly thermalized before addition of the second C_2H_4 ligand. The question is whether reaction (11) is exothermic.

$$Ag_2{}^+(C_2H_4) + C_2H_4 \rightarrow Ag^+(C_2H_4)_2 + Ag \quad (11)$$

$$Ag_2{}^+(C_2H_4) \rightarrow Ag_2{}^+ + C_2H_4 \quad (11a)$$

$$Ag_2{}^+ \rightarrow Ag^+ + Ag \quad (11b)$$

$$Ag^+ + C_2H_4 \rightarrow Ag^+(C_2H_4) \quad (11c)$$

$$Ag_2{}^+(C_2H_4) + C_2H_4 \rightarrow Ag^+(C_2H_4)_2 \quad (11d)$$

This yields the relationship ΔH_{rxn} (11) = ΔH_{rxn} (11a) + $D_0(Ag^+–Ag)$ + ΔH_{rxn} (11c) + ΔH_{rxn} (11d), or ΔH_{rxn} (11) = $D_0(Ag^+–Ag) - 37.6$ kcal/mol. The values for

reactions (11a), (11b), and (11c) were taken from Table 1. Hence, for $D_0(Ag^+–Ag) < 37.6$ kcal/mol, reaction (11) will be exothermic. Thus, it appears that thermochemistry is sufficient to explain the observation that two C_2H_4 ligands are required to dissociate Ag_2^+ as observed experimentally.

Further support for this interpretation comes from some high temperature measurements on the Ag_2^+/C_2H_4 system. Above 725 K only Ag_2^+ and $Ag_2^+(C_2H_4)$ are observed in the mass spectrum and no dissociation products are observed under our signal to noise constraints. This observation makes sense because under the equilibrium conditions of the experiment only an extremely small amount of $Ag_2^+(C_2H_4)_2$ is formed. However, at temperatures between 740 K and 800 K the dissociation reaction reappears. In this instance, however, the reaction has a positive temperature dependence:

$$Ag_2^+ + C_2H_4 \xrightarrow{k_r(T)} Ag^+(C_2H_4) + Ag \quad (12)$$

A plot of $\ln(k_r)$ versus $1/T$ is given in Fig. 5. From an Arrhenius analysis of this data, an activation energy is obtained of E_a (12) = 3.5 ± 0.3 kcal/mol. No configuration energy barrier above the reaction asymptote is expected for this reaction. Therefore, the activation energy is a good measure of the endothermicity of the reaction. From our analysis above (reactions (10), (10a) and (10b)), we suggested reaction (12) should be endothermic by 4.0 ± 3.7 kcal/mol provided $D_0(Ag^+–Ag)$ is about 36 kcal/mol. This is very good agreement and strongly supports the experimental value of Beutel et al. [48] for $D_0(Ag^+–Ag)$ and suggests the value of Kruckeburg et al. [49] of 40.1 ± 2.0 kcal/mol is slightly high.

The next issue to explain is the negative temperature dependence found for the rate constants of reactions (3) and (4). We will consider reaction (3) first since it is simpler. The reaction rate constant is,

$$k_{r3}(T) = k_{coll3}\omega_3(T) \quad (13)$$

where k_{coll3} is the collision rate constant given by Langevin theory and $\omega_3(T)$ is the reaction probability per collision. If we have an orbiting (collisional) transition state leading

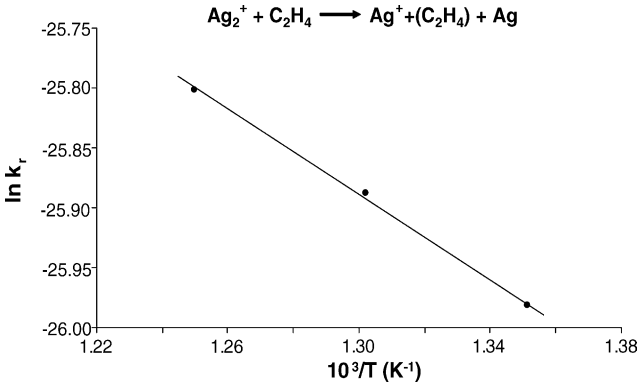

Fig. 5. Plot of $\ln(k_r)$ vs. $1/T$ for the dissociation reaction $Ag_2^+ + C_2H_4 \rightarrow Ag^+(C_2H_4) + Ag$. The line is a least-squares fitting to the data that yields a slope that is proportional to the activation energy of the reaction. The temperature range is 740–800 K.

to the $[Ag_2^+(C_3H_6)]^*$ activated intermediate, another OTS leading to $Ag^+(C_3H_6) + Ag$ products and the possibility of a tight transition state somewhere between the two OTS's, then phase space theory gives Eq. (8) for the microcanonical reaction probability, $\omega_{PST}(E, J)$. This probability has two useful limits: first $N^P_{OTS} >> N_{TTS}$, yielding Eq. (14).

$$\omega_{PST}(E, J) = \frac{N_{TTS}}{N^R_{OTS}} \quad (14)$$

This limit holds for tight transition states with energies near or above the product asymptotic energy. The opposite extreme, $N^P_{OTS} << N_{TTS}$, yields Eq. (15).

$$\omega_{PST}(E, J) = \frac{N^P_{OTS}}{N^P_{OTS} + N^R_{OTS}} \quad (15)$$

This limit holds for a TTS at energies significantly below the product asymptotic energy. The values of N^R_{OTS} and N^P_{OTS} can be readily obtained using well-known phase space theory methods [57,58]. However, in order to evaluate the possible importance of a tight transition state, we needed to get an approximate set of rotational constants and vibrational frequencies. We did this by starting with the structure of the $Ag_2^+(C_3H_6)$ complex obtained from DFT [45], fixing all coordinates except the Ag^+–Ag bond distance, stretching the Ag^+–Ag bond until a maximum was obtained at a distance of 7.03 Å, then relaxing all coordinates except the Ag^+–Ag distance and finding the minimum energy structure. This process allowed us to generate the necessary parameters and yielded one imaginary vibrational frequency corresponding to the stretching of the Ag^+–Ag bond. We realize this is not a proper way to find a TTS but the parameters obtained did allow us to evaluate if a TTS was operating in this reaction system.

The first calculation we did was to assume the TTS was rate limiting (Eq. (14)). We varied the energy of the TTS relative to the reactant energy asymptote until a best fit to the data was obtained. This result is given as the red data and line in Fig. 6a, and corresponds to a TTS 0.17 eV below the reaction asymptotic energy. It is clear that the magnitude of $\omega(T)$ is relatively well-reproduced but the variation of $\omega(T)$ with temperature is poorly reproduced.

The second calculation ignored the TTS completely (Eq. (15)). In this case the reaction exothermicity was varied until a best fit was obtained. These results are given as the blue data and line in Fig. 6a. In this instance, a relatively good fit to both the magnitude of $\omega(T)$ and its variation with T is obtained for ΔH_{rxn} (3) = −0.15 eV (−3.5 kcal/mol). This is a very interesting result in that both the kinetics are well fit and the predicted ΔH_{rxn} (3) is essentially equal to the experimental value discussed earlier.

In order to see whether this fit could be improved, we used the general formula for $\omega(T)$ and varied the energy of the TTS over a wide range of values. The results are given in Fig. 6b. For a TTS at the reactant energy, the reaction is essentially shut down and a slight positive energy dependence

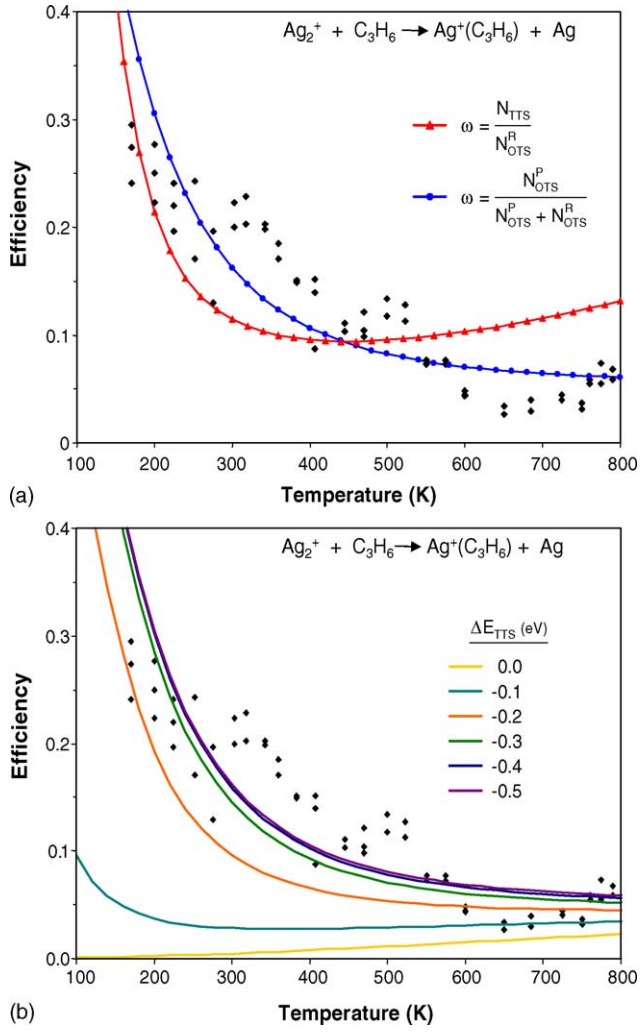

Fig. 6. Plots of reaction efficiency vs. temperature for the reaction $Ag_2^+ + C_3H_6 \rightarrow Ag^+(C_3H_6) + Ag$. The data are shown as the filled blank diamonds (♦). In panel (a) the red curve and points has the tight transition state as rate limiting (Eq. (14)) and the blue curve and points has the product orbiting transition state rate limiting (Eq. (15)). In panel (b) the general form for the reaction efficiency is used (Eq. (8)) and the energy of the TTS relative to the reactant asymptote energy is varied.

is observed. As the energy of the TTS is dropped, the calculation improves until at $E_{TTS} = -0.4$ eV there is no further change and the Eq. (15) limiting case is reproduced. A value between -0.2 eV and -0.3 eV might slightly improve the fit to experiment but no obvious advantage is gained by including the TTS. For reference, the $Ag_2^+(C_3H_6)$ adduct is bound by an energy of -28.1 ± 1.5 kcal/mol (-1.24 eV) relative to the $Ag_2^+ + C_3H_6$ asymptote.

This is an interesting result and not in line with prior observations of negative temperature dependence. In a typical case, a TTS would be located below, but near in energy, to the entrance channel and the product OTS would be much lower in energy. However, in the current case a TTS has little impact on the kinetics and the negative temperature dependence arises from the interplay of the OTS in the entrance channel and the OTS in the product channel. This occurs for

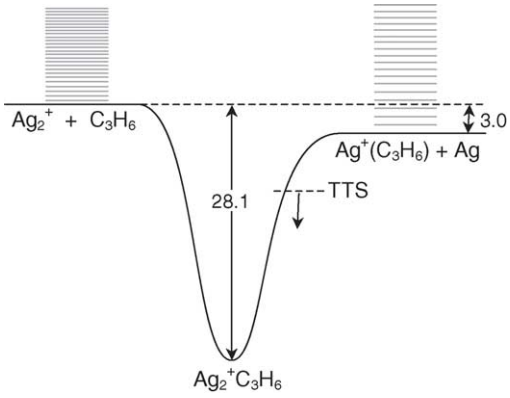

Fig. 7. A schematic potential energy surface for the reaction $Ag_2^+ + C_3H_6 \rightarrow Ag^+(C_3H_6) + Ag$ is given. The density of states for the reactant and product OTS's are shown as the stacks of horizontal lines.

two reasons. First, the reaction is only mildly exothermic. Hence, the density of states in the product channel does not completely dominate in the temperature range of the experiment (300–800 K). Second, and equally important, is the fact that one of the products is a silver atom. Since this atom can only support translational states, the density of states in the product channel increases more slowly with energy than in the entrance channel where polyatomic and diatomic species are involved. This point is made schematically in Fig. 7. As discussed above, the TTS, if it occurs, is located at least 9 kcal/mol below the entrance asymptote.

The results for the ethene system are analogous. The major difference is the reaction is about a factor of 10 less efficient. However, the reaction does display a negative temperature dependence. The same strategy we employed for the simpler C_3H_6 system will be used here. First, we assume the TTS is rate limiting (Eq. (14)). The best fit to the data is given by the red line in Fig. 8a. The magnitude of the reaction efficiencies is about right for a TTS = 0.10 eV below the reactant asymptotic energy but the variation with temperature is clearly wrong. Going to the opposite extreme where the product OTS is rate limiting (Eq. (15)) yields the blue curve in Fig. 8a as a best fit to the data. The ΔH_{rxn} was varied and a final best fit value of -0.14 eV (-3.2 kcal/mol) was obtained. Both the shape and the magnitude of the reaction efficiencies are well matched. In an effort to see if any value of a TTS could improve this result, we used the general form of the reaction efficiency (Eq. (8)) and let the energy of the TTS vary. The results are given in Fig. 8b. It is apparent that no improvement is obtained for any TTS energy.

A question of why the reaction efficiencies for the ethene system are a factor of 10 less efficient than the propene system needs to be addressed. Both reactions are about 3 kcal/mol exoergic according to both independent thermochemistry measurements and PST estimates (these data are shown in Table 2). However, in the ethene case, the reactants are composed of two polyatomic molecules ($Ag_2^+(C_2H_4) + C_2H_4$) while in the propene case a polyatomic/diatomic pair are involved ($Ag_2^+ + C_3H_6$). Therefore, the density of states in the

Table 2
Summary of fitting results for $Ag_2^+(L)_{n-1} + L \rightleftarrows Ag^+(L)_n + Ag$ kinetic experiments[a]

	L = C_2H_4 (n = 2)			L = C_3H_6 (n = 1)		
	Experiment[b]	DFT[c]	PST[d]	Experiment[b]	DFT[c]	PST[d]
ΔE_{TTS}	–	–	<9.0	–	–	<−9.0
ΔH_{rxn}	−1.4 ± 3.5	−1.56	−3.5	−3.0 ± 3.7	∼0	−3.4

[a] In units of kcal/mol. All energies are relative to the separated reactants.
[b] Reaction exothermicity calculated using experimental bond energies.
[c] Theoretical exothermicity were calculated using DFT.
[d] Reaction exothermicity and energy of tight transition state which gave a best fit to the temperature-dependent rate data in phase space calculations.

reactants OTS for the ethene case will increases much faster with energy than for the propene. Both reactions have an atom and a polyatomic molecule as products so the density of states in the product channel will be similar for the two systems. The net result is a significantly less efficient reaction for ethene than for propene, consistent with the necessity of two ethene ligand additions and only one propene ligand addition needed to dissociate Ag_2^+.

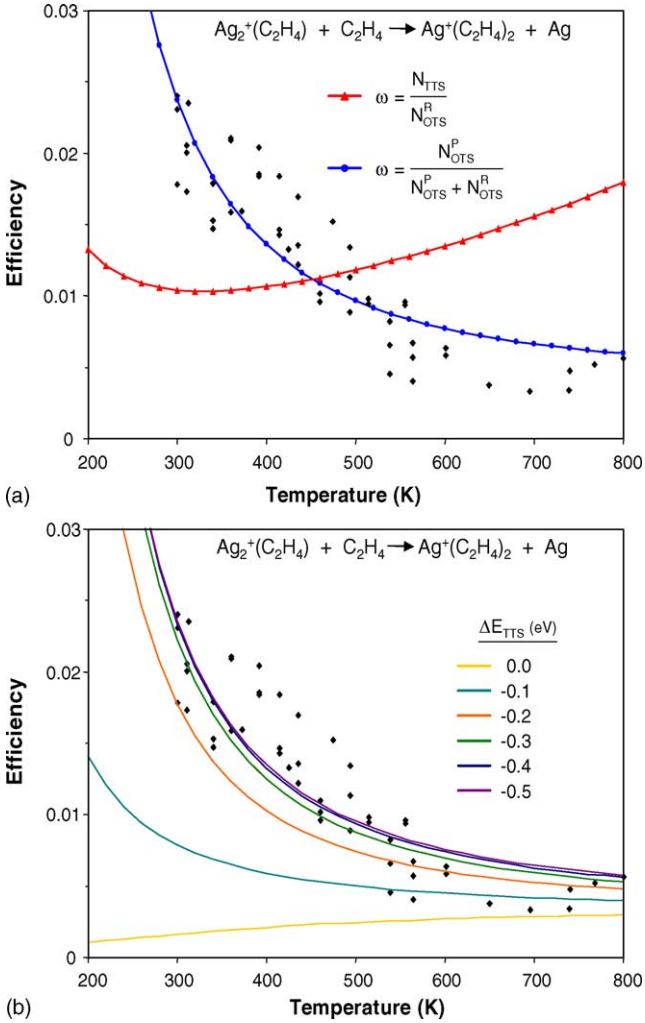

Fig. 8. Plots of reaction efficiency vs. temperature for the reaction $Ag_2^+(C_2H_4) + C_2H_4 \rightarrow Ag^+(C_2H_4)_2 + Ag$. The data are shown as the filled blank diamonds (♦). In panel (a) the red curve and points has the tight transition state as rate limiting (Eq. (14)) and the blue curve and points has the product orbiting transition state rate limiting (Eq. (15)). In panel (b) the general form for the reaction efficiency is used (Eq. (8)) and the energy of the TTS relative to the reactant asymptote energy is varied.

7. Conclusions

Addition of a single C_3H_6 ligand to Ag_2^+ results in cleavage of the Ag^+–Ag bond to form $Ag^+(C_3H_6) + Ag$. Addition of two C_2H_4 ligands is required for Ag_2^+ dissociation to form $Ag^+(C_2H_4)_2$ below 740 K.

At temperatures above 740 K, dissociation of Ag_2^+ with a single C_2H_4 ligand becomes observable and Arrhenius parameters are obtained. The Arrhenius activation energy measured is in good agreement with the reaction endothermicity.

Experimental rate constants for dissociating the Ag_2^+ ion gave negative temperature dependencies for both systems. In both case, the results could be fit quantitatively using phase space theory. The orbiting (loose) TS in the exit channel was rate limiting in both cases. No evidence was found for a tight TS along the reaction coordinate.

The reaction exothermicities required for the PST fits to the rate data (∼3 kcal/mol) are in excellent agreement with estimates from independent thermochemical measurements.

Acknowledgements

The support of the Air Force Office of Scientific Research under grants F 49620-01-1-0459 and F 49620-03-1-0046 is gratefully acknowledged. Additionally, M.J.M. would like to thank J.E. Bushnell for helpful discussions regarding interpretation of the kinetic data presented in this work.

Appendix A. Supplementary data

Supplementary data associated with this article can be found, in the online version, at doi:10.1016/j.ijms.2004.12.025.

References

[1] (a) M.B. Knickelbein, Annu. Rev. Phys. Chem. 50 (1999) 79;
(b) B.S. Freiser (Ed.), Organometallic Ion Chemistry, Kluwer Academic Publishers, Dordrecht, The Netherlands, 1996;
(c) D.H. Russell (Ed.), Gas Phase Inorganic Chemistry, Plenum, New York, 1989;
(d) R.R. Squires, Chem. Rev. 87 (1987) 623;
(e) K. Eller, H. Schwarz, Chem. Rev. 91 (1991) 1121.

[2] P.R. Kemper, J. Bushnell, G. von Helden, M.T. Bowers, J. Phys. Chem. 97 (1993) 52.

[3] P.R. Kemper, J. Bushnell, P. van Koppen, M.T. Bowers, J. Phys. Chem. 97 (1993) 1810.

[4] J.E. Bushnell, P.R. Kemper, M.T. Bowers, J. Phys. Chem. 97 (1993) 11628.

[5] J.E. Bushnell, P.R. Kemper, P. Maitre, M.T. Bowers, J. Am. Chem. Soc. 116 (1994) 9710.

[6] J.E. Bushnell, P.R. Kemper, M.T. Bowers, J. Phys. Chem. 99 (1995) 15602.

[7] P.R. Kemper, P. Weis, M.T. Bowers, Int. J. Mass Spectrom. Ion Process 160 (1997) 17.

[8] P. Weis, P.R. Kemper, M.T. Bowers, J. Phys. Chem. A 101 (1997) 2809.

[9] J.E. Bushnell, P. Maitre, P.R. Kemper, M.T. Bowers, J. Chem. Phys. 106 (1997) 10153.

[10] P.R. Kemper, P. Weis, M.T. Bowers, Chem. Phys. Lett. 293 (1998) 503.

[11] P.R. Kemper, P. Weis, M.T. Bowers, P. Maitre, J. Am. Chem. Soc. 120 (1998) 13494.

[12] M.J. Manard, J.E. Bushnell, S.L. Bernstein, M.T. Bowers, J. Phys. Chem. A 106 (2002) 10027.

[13] M.R. Sievers, P.B. Armentrout, J. Phys. Chem. 99 (1995) 8135.

[14] F.A. Khan, D.E. Clemmer, R.H. Schultz, P.B. Armentrout, J. Phys. Chem. 97 (1993) 7978.

[15] R.H. Schultz, K.C. Crellin, P.B. Armentrout, J. Am. Chem. Soc. 113 (1991) 8590.

[16] S. Goebel, C.L. Haynes, F.A. Khan, P.B. Armentrout, J. Am. Chem. Soc. 117 (1995) 6994.

[17] F.A. Khan, D.L. Steele, P.B. Armentrout, J. Phys. Chem. 99 (1995) 7819.

[18] F. Meyer, Y.M. Chen, P.B. Armentrout, J. Am. Chem. Soc. 117 (1995) 4071.

[19] M.J. Manard, P.R. Kemper, M.T. Bowers, Int. J. Mass Spectrom. 228 (2003) 865.

[20] (a) D. Vardhan, R. Liyanage, P.B. Armentrout, J. Chem. Phys. 119 (2003) 4166;
(b) X.G. Zhang, P.B. Armentrout, J. Phys. Chem. A 107 (2003) 8904.

[21] P.A.M. van Koppen, P.R. Kemper, J.E. Bushnell, M.T. Bowers, J. Am. Chem. Soc. 117 (1995) 2098.

[22] Q. Zhang, P.R. Kemper, S.K. Shin, M.T. Bowers, Int. J. Mass Spectrom. 204 (2001) 281.

[23] Q. Zhang, P.R. Kemper, M.T. Bowers, Int. J. Mass Spectrom. 210 (2001) 265.

[24] P.A.M. van Koppen, J.K. Perry, P.R. Kemper, J.E. Bushnell, M.T. Bowers, Int. J. Mass Spectrom. 187 (1999) 989.

[25] P.R. Kemper, M.T. Hsu, M.T. Bowers, J. Phys. Chem. 95 (1991) 10600.

[26] J.E. Bushnell, P.R. Kemper, M.T. Bowers, J. Phys. Chem. 98 (1994) 2044.

[27] P.R. Kemper, J. Bushnell, M.T. Bowers, G.I. Gellene, J. Phys. Chem. A 102 (1998) 8590.

[28] P.A.M. van Koppen, M.T. Bowers, C.L. Haynes, P.B. Armentrout, J. Am. Chem. Soc. 120 (1998) 5704.

[29] P. Weis, P.R. Kemper, M.T. Bowers, J. Phys. Chem. A 101 (1997) 8207.

[30] J. Allison, R.B. Freas, D.P. Ridge, J. Am. Chem. Soc. 101 (1979) 1332.

[31] C.J. Carpenter, P.A.M. van Koppen, M.T. Bowers, J. Am. Chem. Soc. 117 (1995) 10976.

[32] J. Gidden, P.A.M. van Koppen, M.T. Bowers, J. Am. Chem. Soc. 119 (1997) 3935.

[33] For reviews, see: P.B. Armentrout, in: J.A. Davies, P.L. Watson, A. Greenberg, J.F. Liebman (Eds.), Selective Hydrocarbon Activation: Principles and Progress, Wiley-VCH, New York, 1990, p. 467;
P.B. Armentrout, in: D.H. Russell (Ed.), Gas Phase Inorganic Chemistry, Plenum, New York, 1989, 1 ;
P.B. Armentrout, J.L. Beauchamp, Accounts Chem Res 22 (1989) 315.

[34] For reviews, see: P.B. Armentrout, Science 251 (1991) 175;
P.B. Armentrout, Annu. Rev. Phys. Chem. 41 (1990) 313.

[35] (a) P.B. Armentrout, M.R. Sievers, J. Phys. Chem. A 107 (2003) 4396;
(b) M.R. Sievers, P.B. Armentrout, Organometallics 22 (2003) 2599.

[36] Y.M. Chen, P.B. Armentrout, J. Phys. Chem. 99 (1995) 11424.

[37] B.C. Guo, A.W. Castleman, Chem. Phys. Lett. 181 (1991) 16.

[38] J. Kaneti, L.C.P.M. de Smet, R. Boom, H. Zuilhof, E.J.R. Sudholter, J. Phys. Chem. A 106 (2002) 11197.

[39] Y.C. Huang, P.H. Su, C.S. Yeh, B. Chem. Soc. Jpn. 74 (2001) 677.

[40] R.H. Hertwig, W. Koch, D. Schroder, H. Schwarz, J. Hrusak, P. Schwerdtfeger, J. Phys. Chem. 100 (1996) 12253.

[41] N.L. Ma, Chem. Phys. Lett. 297 (1998) 230.

[42] J.S. Dewar, B. Soc. Chim. Fr. 18 (1951) 71.

[43] T. Ziegler, A. Rauk, Inorg. Chem. 18 (1979) 1558.

[44] (a) J.G. Serafin, A.C. Liu, S.R. Seyedmonir, J. Mol. Catal. A-Chem. 131 (1998) 157;
(b) D.J. Sajkowski, M. Boudart, Catal. Rev. 29 (1987) 325;
(c) A.L. de Oliveira, A. Wolf, F. Schuth, Catal. Lett. 73 (2001) 157.

[45] M.J. Manard, P.R. Kemper, M.T. Bowers, Int. J. Mass. Spectrom. 241 (2005) 109.

[46] P.R. Kemper, M.T. Bowers, J. Am. Soc. Mass Spectrom. 1 (1990) 197.

[47] D.F. Liu, T. Wyttenbach, C.J. Carpenter, M.T. Bowers, J. Am. Chem. Soc. 126 (2004) 3261.

[48] V. Beutel, G.L. Bhale, M. Kuhn, W. Demtroder, Chem. Phys. Lett. 185 (1991) 313.

[49] S. Krückeberg, G. Dietrich, K. Lützenkirchen, L. Schweikhard, C. Walther, J. Ziegler, J. Chem. Phys. 110 (1999) 7216.

[50] (a) P. Hohenberg, W. Kohn, Phys. Rev. B 136 (1964) 864;
(b) W. Kohn, L.J. Sham, Phys. Rev. 140 (1965) 1133.

[51] P.J. Stephens, F.J. Devlin, C.F. Chabalowski, M.J. Frisch, J. Phys. Chem. 98 (1994) 11623.

[52] (a) A.D. Becke, J. Chem. Phys. 98 (1993) 5648;
(b) A.D. Becke, Phys Rev A 38 (1988) 3098.

[53] Gaussian 98, Revision A.7, M.J. Frisch, G.W. Trucks, H.B. Schlegel, G.E. Scuseria, M.A. Robb, J.R. Cheeseman, V.G. Zakrzewski, J.A. Montgomery Jr., R.E. Stratmann, J.C. Burant, S. Dapprich, J.M. Millam, A.D. Daniels, K.N. Kudin, M.C. Strain, O. Farkas, J. Tomasi, V. Barone, M. Cossi, R. Cammi, B. Mennucci, C. Pomelli, C. Adamo, S. Clifford, J. Ochterski, G.A. Petersson, P.Y. Ayala, Q. Cui, K. Morokuma, D.K. Malick, A.D. Rabuck, K. Raghavachari, J.B. Foresman, J. Cioslowski, J.V. Ortiz, A.G. Baboul, B.B. Stefanov, G. Liu, A. Liashenko, P. Piskorz, I. Komaromi, R. Gomperts, R.L. Martin, D.J. Fox, T. Keith, M.A. Al-Laham, C.Y. Peng, A. Nanayakkara, C. Gonzalez, M. Challacombe, P.M.W. Gill, B. Johnson, W. Chen, M.W. Wong, J.L. Andres, C. Gonzalez, M. Head-Gordon, E.S. Replogle, J.A. Pople, Gaussian Inc., Pittsburgh, PA, 1998.

[54] (a) M.M. Francl, W.J. Pietro, W.J. Hehre, J.S. Binkley, M.S. Gordon, D.J. Defrees, J.A. Pople, J. Chem. Phys. 77 (1982) 3654;
(b) T. Clark, J. Chandrasekhar, G.W. Spitznagel, P.V. Schleyer, J. Comput. Chem. 4 (1983) 294;
(c) R. Krishnan, J.S. Binkley, R. Seeger, J.A. Pople, J. Chem. Phys. 72 (1980) 650;

(d) P.M.W. Gill, B.G. Johnson, J.A. Pople, M.J. Frisch, Chem. Phys. Lett. 197 (1992) 499.
[55] (a) P.J. Hay, W.R. Wadt, J. Chem. Phys. 82 (1985) 270;
(b) W.R. Wadt, P.J. Hay, J. Chem. Phys. 82 (1985) 284;
(c) P.J. Hay, W.R. Wadt, J. Chem. Phys. 82 (1985) 299.
[56] Basis sets were obtained from the Extensible Computational Chemistry Environment Basis Set Database, Version 10/21/03, as developed and distributed by the Molecular Science Computing Facility, Environmental and Molecular Sciences Laboratory which is part of the Pacific Northwest Laboratory, P.O. Box 999, Richland, Washington 99352, USA, and funded by the U.S. Department of Energy. The Pacific Northwest Laboratory is a multi-program laboratory operated by Battelle Memorial Institute for the U.S. Department of Energy under contract DE-AC06-76RLO 1830. Contact David Feller or Karen Schuchardt for further information.
[57] (a) W.J. Chesnavich, M.T. Bowers, Prog. React. Kinet. 11 (1982) 137;
(b) W.J. Chesnavich, L. Bass, T. Su, M.T. Bowers, J. Chem. Phys. 74 (1981) 2228;
(c) W.J. Chesnavich, M.T. Bowers, J. Chem. Phys. 68 (1978) 901;
(d) W.J. Chesnavich, M.T. Bowers, J. Am. Chem. Soc. 98 (1976) 8301.
[58] For some examples of applications of PST, see: (a) Q. Zhang, C.J. Carpenter, P.R. Kemper, M.T. Bowers J. Am. Chem. Soc. 125 (2003) 3341;
(b) S.T. Graul, C.J. Carpenter, J.E. Bushnell, P.A.M. van Koppen, M.T. Bowers, J. Am. Chem. Soc. 120 (1998) 6785;
(c) L.M. Bass, M.T. Bowers, J. Chem. Phys. 86 (1987) 2611;
(d) A.J. Illies, M.F. Jarrold, L.M. Bass, M.T. Bowers, J. Am. Chem. Soc. 105 (1983) 5775.